Published in final edited form as:
Circ Res. 2011 September 16; 109(7): 775–782. doi:10.1161/CIRCRESAHA.111.247957.

Fibroblast growth factor homologous factor 13 regulates Na^+ channels and conduction velocity in murine heart

Chuan Wang, **Jessica A. Hennessey**, **Robert D. Kirkton**, **Chaojian Wang**, **Victoria Graham**, **Ram S. Puranam**, **Paul B. Rosenberg**, **Nenad Bursac**, and **Geoffrey S. Pitt**
Departments of Medicine/Cardiology (C.W., J.A.H., C.W., V.G., P.B.R., G.S.P.), Biomedical Engineering (R.D.K., N.B.), Neurobiology (R.S.P., G.S.P.), Medicine (R.S.P.), and Pharmacology and Molecular Cancer Biology (G.S.P.), Duke University Medical Center, Durham, North Carolina, USA

Abstract

Rationale—Fibroblast growth factor homologous factors (FHFs), a subfamily of fibroblast growth factors (FGFs) that are incapable of functioning as growth factors, are intracellular modulators of Na^+ channels and have been linked to neurodegenerative diseases. Although certain FHFs have been found in embryonic heart, they have not been reported in adult heart, and they have not been shown to regulate endogenous cardiac Na^+ channels nor participate in cardiac pathophysiology.

Objective—We tested whether FHFs regulate Na^+ channels in murine heart.

Methods and Results—We demonstrated that isoforms of FGF13 are the predominant FHFs in adult mouse ventricular myocytes. FGF13 binds directly to, and co-localizes with the Na 1.5 Na^+ V channel in the sarcolemma of adult mouse ventricular myocytes. Knockdown of FGF13 in adult mouse ventricular myocytes revealed a loss-of-function of $Na_V1.5$: reduced Na^+ current (I_{Na}) density, decreased Na^+ channel availability, and slowed I_{Na} recovery from inactivation. Cell surface biotinylation experiments showed a ~45% reduction in $Na_V1.5$ protein at the sarcolemma after FGF13 knockdown, whereas no changes in whole-cell $Na_V1.5$ protein nor mRNA level were observed. Optical imaging in neonatal rat ventricular myocyte monolayers demonstrated slowed conduction velocity and a reduced maximum capture rate after FGF13 knockdown.

Conclusion—These findings show that FHFs are potent regulators of Na^+ channels in adult ventricular myocytes and suggest that loss-of-function mutations in FHFs may underlie a similar set of cardiac arrhythmias and cardiomyopathies that result from $Na_V1.5$ loss-of-function mutations.

Keywords

Fibroblast growth factor homologous factor; Fibroblast growth factor; Voltage-gated Na^+ channels; Channel trafficking

Address correspondence to: Geoffrey S. Pitt, Box 103030 Med Center, Duke University, Durham, North Carolina 27710, USA. Phone: 919.668.7641; Fax 919.613.5145; geoffrey.pitt@duke.edu..

Disclosures None.

Introduction

The four fibroblast growth factor homologous factors (FHFs), a subset of the fibroblast growth factor (FGF) family, have received increasing attention for their unanticipated modulation of neuronal voltage-gated Na^+ channels (VGSCs) and regulation of neuronal excitability. Although FHFs are potentially important regulators of cardiac VGSCs, the function of FHFs in cardiac myocytes has not been investigated and would provide insight into arrhythmogenesis caused by changes in sodium channel function. FHFs were originally named because of their similarity with FGFs, but several defining features of the FHFs (FGF11, FGF12, FGF13, and FGF14) set them apart from other FGFs.[1] First, only the central core domain of each FHF shares homology with the FGF superfamily.[1] Outside of this core domain, FHFs have extended N- and C-termini compared to FGFs. For each FHF, these N-termini, encoded by alternatively spliced first exons, provide significant diversity.[2] An additional feature distinguishing them from FGFs is that FHF N-termini lack signal sequences and FHFs are thus not secreted. While other non-secreted FGFs, such as FGF-9, are released after cell damage and activate cell surface FGF receptors on target cells, FHFs are incapable of stimulating FGF receptors.[3] Thus, FHFs do not function as secreted growth factors or morphogens. Rather, these intracellular proteins bind to the intracellular C termini of VGSCs and modulate channel function.[4]

All FHFs are expressed most abundantly in the brain[1] and several loss-of-function mutations have established FGF14 as the locus for spinocerebellar ataxia 27 (SCA27).[5-8] The prototypical SCA27 mutant $FGF14^{F145S}$ reduces Na^+ channels at the axon initial segment, diminishes Na^+ currents (I_{Na}), and dampens excitability in a dominant negative manner when expressed in cultured hippocampal neurons.[8]

Although not yet investigated, analogous regulation of cardiac Na^+ channels by FHFs and dysregulation by mutant FHFs could underlie cardiac physiology and pathophysiology, respectively. Na^+ channel dysfunction is central to various inherited arrhythmias such as Long QT Syndrome and Brugada Syndrome. FHF regulation of extraneuronal Na^+ channels has received little attention, however, despite evidence that certain FHF family members are expressed in heart[2] and that FGF12 and FGF14 can modulate gating kinetics of the cardiac Na^+ channel Na 1.5 in a heterologous expression system.[9, 10] V Whether FHFs affect $Na_V1.5$ in cardiac myocytes and whether loss of function alters myocyte excitability has not been addressed. Further, certain FHFs appear to interact with only a subset of VGSCs,[9] suggesting the need for analyzing specific FHFs in the context of the VGSC expressed in a specific cell type.

Here, we investigated whether FHFs are capable of modulating I_{Na} in adult mouse ventricular myocytes. We show that: specific FGF13 isoforms are the major FHFs expressed in mouse heart and they can bind to and modulate cardiac $Na_V1.5$ Na^+ channel function and membrane expression, leading to changes in cardiac conduction properties. This work identifies FHFs as potent modulators of cardiac I_{Na} and suggests FHF mediated dysregulation of I_{Na} may have proarrhythmic effects in heart.

Methods

Mice and rats. Animals were handled according to National Institutes of Health Guide for the Care and Use of Laboratory Animals and approved by Duke University Animal Care and Welfare Committee.

Antibodies: The anti-FGF13 antibody (raised in rabbit) was designed against a peptide (RSVSGVLNGGKSMSHNEST) in the C terminus of the protein and was affinity-purified (Yenzym).

Isolation, Culture and Adenoviral Infection of Adult Mouse Ventricular myocytes: Myocytes were isolated from C57/BL6 mice, basically as described, with minor modifications as indicated in the expanded Methods [11].

Immunostaining and confocal microscopy: was performed as described [11].

Biotinylation: Cultured adult mice ventricular myocytes were incubated in 1 mg/ml sulfo-NHS-SS-Biotin (Thermo Scientific) in PBS for 30 minutes at 4 °C, washed, lysed, and biotinylated proteins were purified with NeutrAvidin agarose resin (Thermo Scientific).

GST pull down: The human $Na_V1.5$ C-terminus (aa 1773-2018) was fused to GST in pGEX-4T.

Optical Mapping of Action Potential Propagation: was performed as described[12, 13].

Electrophysiology: Na^+ currents (I_{Na}) in adult mice ventricular myocytes were recorded using the whole-cell patch clamp technique as previously described.[14-16].

Statistical analyses: Results are presented as means ± standard error; the statistical significance of differences between groups was assessed using either a two-tailed Student's *t* test or one-way ANOVA and was set at $P< 0.05$.

Results

We investigated which FHF transcripts were most abundant in the adult mouse heart. To exclude contamination by neuronal FHFs, we used isolated adult mouse ventricular myocytes. Various alternatively spliced FGF11 and FGF13 transcripts were previously identified in both embryonic and adult mouse heart,[2] but their relative expression levels have not been assessed. We therefore designed a quantitative RT-PCR (qPCR) strategy with isoform specific primers (Figure 1A and Online Table I) to define the relative expressions levels of all FHF isoforms in isolated adult mouse ventricular myocytes. As seen in Figure 1B, FGF13-VY was most abundant and other FGF13 isoforms were expressed at lower levels, except for FGF13-U, which was barely detectable. Transcripts for FGF11, FGF12, and FGF14-A were also expressed at very low levels; the level of message for FGF14-B was detectable, but still at low levels compared to FGF13-VY. To corroborate our qPCR findings, we investigated the protein expression of each FHF by immunoblot of lysates from isolated adult mouse ventricular myocytes. As shown in Figure 1C, only FGF13 was detected by immunoblot using a novel polyclonal antibody (see Online Figure IA and see below). The FGF13 in heart migrated at about 29 kDa, consistent with M_w of the FGF13-VY variant that was most abundant by qPCR. To confirm that the FGF11, FGF12, and FGF14 antibodies were capable of detecting endogenous FHFs, we immunoblotted lysates from whole brain and observed that all four FHFs were detectable (Figure 1C). The relative abundance of FHF proteins in brain was consistent with their respective mRNA levels, as quantified by qPCR (Online Figure II). In brain, the FGF13 antibody detected a band that migrated faster than the band observed in lysates from ventricular cardiomyocytes. Consistent with that pattern, qPCR for FGF13 variants in mouse brain showed that the FGF13-S isoform (predicted M_w of 27.6 kDa) was the most abundant FGF13 mRNA. The use of different antibodies, each of which has its distinct affinity for its specific target, precludes a direct quantitative assessment of protein abundance. Nevertheless, the correlations between protein abundance by immunoblot and mRNA expression by qPCR in both brain and heart suggest that FGF13 is the most abundant FHF in heart, and any FHF regulation of cardiac Na^+ channels in adult mouse ventricular myocytes would be mediated predominantly by FGF13 isoforms. Although previous heterologous expression system data

have suggested that FGF12 and FGF14 are capable of modulating $Na_V1.5$,[9, 10] we therefore concentrated our subsequent studies exclusively on FGF13.

To characterize FGF13 in ventricular myocytes we generated a polyclonal antibody against a peptide in the C terminus of FGF13, designed to recognize all FGF13 isoforms (Online Figure IA). The antibody was specific for FGF13, recognizing FGF13-VY expressed in tsA201 cells but not FGF12 or FGF14, as shown in Online Figure IB. Having demonstrated the antibody's specificity, we tested for the presence of FGF13 in isolated adult mouse ventricular myocytes. Figure 2A shows an immunoblot in which the FGF13 antibody recognizes a major band of ~ 29 kDa (predicted M_w for FGF13-VY is 28.8 kDa). A fainter band is apparent at ~ 26 kDa, which could represent a degradation product, FGF13-V, or FGF13-Y (predicted M_w for FGF13-V and FGF13-Y are 22.3 and 25.6 kDa, respectively). These bands are likely specific, since no signals were observed after addition of the immunizing peptide to the antibody (Figure 2A, right lane). The FGF13 antibody was also able to co-immunoprecipitate $Na_V1.5$ from isolated mouse ventricular myocyte lysates (Figure 2B), suggesting that FGF13 and $Na_V1.5$ are in the same complex. No $Na_V1.5$ was co-immunoprecipitated with a control IgG antibody. This interaction was likely direct, as indicated by pull-down experiments with GST fusion proteins. A GST-fusion protein containing the $Na_V1.5$ C terminus, but not the GST control protein, pulled down the His6-tagged FGF13-VY from lysates of transiently transfected tsA201 cells (Figure 2C); the $Na_V1.5$ CT also pulled down recombinant versions of all the FGF13 isoforms (not shown), suggesting a common site of interaction—the FGF13 core—consistent with studies on other FHF / $Na_V1.x$ interactions.[17] Thus, FGF13 isoforms bind directly to the $Na_V1.5$ C terminus. Immunostaining experiments were performed to assess the expression pattern in single ventricular myocytes and ventricular tissues. Immunocytochemistry on isolated adult mouse ventricular myocytes showed FGF13 co-localized with Nav1.5 at the lateral membrane and intercalated discs (Figure 2D, left panels), which was verified by co-staining with the known marker, ankyrin-G (Figure 2D, right panels).[18] We also noted FGF13 in the nucleus and cytoplasm, which has been previously described in COS cells.[12] Immunohistochemistry on adult mouse ventricle demonstrated no overt transmural gradients of FGF13 in left (Online Figure III) and right ventricle (not shown).

To evaluate the role of endogenous FGF13 in the regulation of cardiac I_{Na}, we knocked down FGF13 in isolated mouse ventricular myocytes with an adenovirus expressing both a shRNA targeting all FGF13 isoforms and GFP (to identify transfected cells). An adenovirus expressing a scrambled shRNA with GFP was employed as a control. Viral infection itself did not affect FGF13 expression as shown by the two myocytes infected with adenovirus expressing a scrambled sequence (Figure 3A, top panels): the level of FGF13 and its overall cellular pattern are similar in the infected cell (as indicated by GFP) and the adjacent non-infected cell (GFP-negative). In contrast, immunostaining with the FGF13 antibody showed that the FGF13 shRNA markedly reduced FGF13 expression compared to control (uninfected) cells or cells infected with a scrambled shRNA (Figure 3A, bottom panels). Almost no sarcolemmal membrane or cytoplasmic FGF13 was visible after shRNA knockdown, although a minor amount of nuclear FGF13 remained. Efficacy of knockdown by the shRNA was also analyzed by qPCR, which showed a 90 ± 3% ($p < 0.01$) reduction in FGF13 mRNA compared to a scrambled control shRNA (Figure 3B), and by immunoblot, which showed 92 ± 2% ($p < 0.01$) reduction in FGF13 protein (Figure 3C-D). Moreover, these data confirmed the specificity of the shRNA, since FGF12 mRNA levels were unaffected (Figure 3B). Having demonstrated the efficiency of knockdown by FGF13 shRNA, I_{Na} was recorded and analyzed in single adult ventricular myocytes infected with FGF13 shRNA, scrambled shRNA, or no treatment control. Figure 3E shows representative families of whole-cell I_{Na} in cardiomyocytes recorded from a holding potential of −120 mV to test potentials between −100 mV and +60 mV in 5-mV increments. Whereas mean whole-

cell capacitance was not significantly altered after FGF13 knockdown, peak current density, measured at −30mV, was reduced by 49 ± 4% ($p < 0.01$) (Table 1 and Figure 3E-F) compared to cells treated with scrambled shRNA or untreated controls.

To determine the mechanisms by which FGF13 knockdown reduced current density in myocytes, we investigated whether FGF13 affected the amount of $Na_V1.5$ at the sarcolemma, altered $Na_V1.5$ gating kinetics, or both. To evaluate the amount of $Na_V1.5$ at the sarcolemma, we labeled cell-surface proteins in isolated myocytes with biotin, lysed the myocytes, and captured biotinylated proteins with NeutrAvidin beads. Sarcolemmal $Na_V1.5$ was then quantified by immunoblot using an anti-$Na_V1.5$ antibody. Transferrin receptor, an endogenous plasma membrane protein, was used to normalize sarcolemmal $Na_V1.5$ among different experiments[19] and GAPDH was used for normalizing total $Na_V1.5$ protein levels. The fractionation was effective since no GAPDH was detected among the biotinylated proteins (not shown). An exemplar experiment is shown in Figure 4A. Quantification of 3 independent experiments (Figure 4B) revealed that knockdown of FGF13 had no effect on the total amount of $Na_V1.5$ in the myocyte lysate (99 ± 8% of control, $p > 0.05$), but reduced surface $Na_V1.5$ by 45 ± 5% ($p < 0.01$, compared to control). In contrast to effect upon surface $Na_V1.5$ protein levels, FGF13 knockdown did not alter $Na_V1.5$ mRNA levels, which were assessed by qPCR (Figure 4C). Together, these data suggest that FGF13 knockdown reduced current density by specifically reducing sarcolemmal $Na_V1.5$ without affecting channel transcription or translation.

To assess whether the reduction in current density after FGF13 knockdown might also be due to effects upon channel gating kinetics, we analyzed Na^+ channel activation, inactivation, and recovery from inactivation in isolated ventricular myocytes. Activation was unaffected by FGF13 knockdown as shown in Figure 4D. Steady-state inactivation was determined using a standard double-pulse protocol and the data fitted by a Boltzmann equation (Figure 4E and Table 1). Knockdown of FGF13 resulted in a hyperpolarized shift in steady-state I_{Na} inactivation, indicating that the fraction of available Na^+ channels was reduced at membrane potentials more depolarized than ~−110 mV. Since the decrease in availability was significant at holding potentials near the resting membrane potential of a ventricular myocyte (i.e., ~ −90 mV), we analyzed how much the contribution of decreased availability contributed to the reduction in current density at a holding potential of −90 mV compared to −130 mV, where availability was unaffected (Figure 4F-G and Table 1). We found that FGF13 knockdown decreased current density by ~ 50% (10.3 ± 0.9 pA/pF *versus* 20.3 ± 2.1 pA/pF, $p < 0.01$) when the myocytes were held at −130 mV, consistent to the observed reduction in $Na_V1.5$ protein at the sarcolemma (see Figure 4B). In contrast, when myocytes were held at −90 mV, FGF13 knockdown reduced current density by 72 % (3.5 ± 0.5 pA/pF *versus* 12.3 ± 2.5 pA/pF, $p < 0.01$), suggesting that current density was decreased not only by the reduced amount of $Na_V1.5$ at the sarcolemma, but also by reduced channel availability. Knockdown of FGF13 also delayed channel recovery from inactivation (Figure 5 and Table 1). Double exponential fits showed that the fast and slow components were significantly slowed compared to control myocytes or myocytes treated with scrambled shRNA (Table 1). Because I_{Na} completely recovered within less than 200 ms in cardiomyocytes of either group, the interpulse interval (3 s) used in the protocols for activation and inactivation was sufficiently long to allow complete recovery. However, the delayed recovery from inactivation in FGF13 knockdown myocytes predicts that at elevated heart rates the insufficient time for recovery would reduce sodium channel availability and thus decrease excitability and slow cardiac conduction.

We therefore tested whether FGF13 knockdown in myocytes affected cardiac conduction properties. We knocked down FGF13 in neonatal rat ventricular myocyte monolayers cultured on fibronectin and analyzed conduction velocity and maximum capture rate by

optical mapping.[9, 10] As shown in Figure 6A and C, conduction velocity was markedly slowed in monolayers after FGF13 knockdown (9.7 ± 1.3 cm/s, $p < 0.001$) compared to control monolayers (18.9 ± 1.1 cm/s) or monolayers infected with the scrambled shRNA (16.7 ± 1.0 cm/s). Action potential duration (Figure 6B and D) was unaffected (206.7 ± 7.7 ms, 189.1 ± 9.7 ms and 206.8 ± 11.4 ms for Control, Scrambled and shRNA, respectively, $p > 0.05$, compared to Control). Maximum capture rate, defined as the maximum rate at which a 1:1 response of monolayers was maintained for at least 30 s of pacing, was significantly reduced after FGF13 knockdown (4.6 ± 0.2 Hz, 4.7 ± 0.2 Hz, and 3.3 ± 0.2 Hz for control, scrambled shRNA, and FGF13 shRNA, respectively, $p < 0.001$, compared to control) (Figure 6E). Taken together, these data suggest that FGF13 knockdown is associated with abnormal cardiac conduction properties due to reduced Na^+ channel current density and delayed recovery from inactivation.

Discussion

This is the first report demonstrating that FHFs affect VGSCs in cardiac myocytes. Although FHFs have well-documented effects upon VGSCs in neurons and FGF14 is the locus for SCA27,[5, 8, 20-24] whether FHFs operate within cardiac myocytes and any consequential effects of FHF actions within myocytes have not been investigated. While previous reports demonstrated that certain FHFs (FGF12 and FGF14) were capable of modulating $Na_V1.5$ in heterologous expression systems,[9, 10] this study demonstrates how endogenous FHFs modulate VGSCs in cardiac myocytes.

We showed that FGF13 is the major FHF in mouse ventricular myocytes and that it has critical roles in modulation of $Na_V1.5$ channel function and membrane expression in myocytes. Knockdown of FGF13 decreased $Na_V1.5$ at the sarcolemma and decreased Na^+ channel availability at holding potentials near the ventricular myocyte resting potential. The combined effects produced a marked reduction in Na^+ channel current density. These results suggest that loss-of-function mutations in cardiac FHFs may be unrecognized causes of cardiac disorders associated with Na^+ channel loss-of-function. Consistent with our data obtained in isolated myocytes, we found that conduction velocity was reduced in neonatal cardiomyocyte monolayers using optical mapping. Although it is likely that this is a result of the reduced current density and/or channel availability seen the single cell experiments, we cannot exclude other mechanisms, such as changes in gap junction properties. Additionally, optical mapping showed a significant decrease in maximum capture rate, likely due to the observed slowing of Na^+ channel recovery from inactivation. Together, these results suggest that loss-of-function mutations in cardiac FHFs may be pro-arrhythmic by lowering the threshold of heart rate for which Na^+ channels can fully recover, and decreasing conduction velocity and maximum capture rate, thereby providing a substrate for re-entrant arrhythmias. Slowed conduction, due to mutations in Na 1.5, is a hallmark of Brugada syndrome,[25] V suggesting that FHFs may be unrecognized and unexplored Brugada syndrome loci, for which identified loci explain only about 30% of patients. While no human mutations in an FHF have yet been associated with an inherited arrhythmia or conduction disorder, our data provide evidence that FHFs might join the growing list of members in the recently coined "sodium channelsome" in the heart,[26] in which mutations in modulators affect cardiac Na^+ channel function and thereby cause a similar set of disorders attributed to mutations in the channels, themselves.

Our data provide other mechanistic insights into how FGF13 regulates cardiac I_{Na}. In addition to affecting channel gating, we observed that FGF13 increases the amount of channel at the sarcolemma without affecting $Na_V1.5$ transcription or translation. This appears analogous to the role that FHFs play in targeting VGSCs to the axon initial segment of neurons,[1, 2] suggesting that regulation of VGSC trafficking by FHFs may be widespread

and opening an interesting avenue for future investigation in the field of channel trafficking. Our co-immunoprecipitation and GST pull-down experiments suggest that FGF13 interacts directly with $Na_V1.5$, as has been reported for other FHF-$Na_V1.x$ pairs. This direct binding is likely responsible for the effects of FGF13 upon channel kinetics, as we recently demonstrated.[27] Whether regulation of trafficking also requires direct interaction between FHFs and $Na_V1.x$ C termini is not known, but a previous report suggests that $Na_V1.x$ C-termini are hotspots for regulation of channel trafficking, through its binding partners (membrane localization of $Na_V1.1$ was augmented by calmodulin, a G protein βγ complex, and a sodium channel β subunit, all of which interact with the channel's C-terminus[28]; and a FGF14 SCA27 causing mutant, which abolished binding of that FHF to $Na_V1.2$, reduced targeting of VGSCs to the axon initial segment[8]) or because of the C-termini themselves (the Y1795H mutation in $Na_V1.5$ reduces current density, whereas Y1795C has increases current density[29]). Whether any or all of these binding partners are concurrently associated with a $Na_V1.x$ C-terminus and thereby confer an integrated form of regulation is not yet known.

We cannot exclude the possibility that FGF13 modulates the channel through other means that we have not explored. Indeed, the widespread cellular distribution of FGF13 hints at other roles for FGF13 in cardiomyocytes, including the modulation of other cardiac ion channels. Of particular interest is prominent nuclear localization of a portion of FGF13, previously also seen for other FHF isoforms in heterologous expression systems.[8, 10] Further, the punctate distribution throughout the cytoplasm suggests that FGF13 plays additional roles in myocyte yet to be described. Those roles may be revealed when a FGF13 knockout model becomes available. While this study characterizes the expression pattern and role of FGF13 in ventricular cardiomyocytes, we did not assess the levels of FGF13 mRNA or protein in the atria or the conduction system. It is possible that different FHFs predominate in other areas of the myocardium and confer different roles.

A significant contribution of this study is that the analyses were performed in cardiac myocytes. Previous experience with other FHFs have shown that data derived from heterologous expression systems do not necessarily reveal the functions of endogenous FHFs in native cell types. Thus, the biochemistry and cellular electrophysiology reported here help advance the understanding of FHF regulation of I_{Na} within cardiac myocytes.

Supplementary Material

Refer to Web version on PubMed Central for supplementary material.

Acknowledgments

We thank J.O. McNamara for helpful discussions and careful reading of the manuscript.

Sources of Funding This work was supported by grants from the National Institutes of Health National Heart, Lung, and Blood Institute (R01 HL71165 and R01 HL088089). G.S. Pitt is supported by an Established Investigator Award from the American Heart Association. J.A. Hennessey is supported by T32-GM007171 from NIH and the Gertrude Elion Mentored Medical Student Research Award.

Abbreviations

(FHF)	Fibroblast growth factor homologous factor
(FGF)	Fibroblast growth factors
(VGSC)	Voltage-gated Na^+ channels

(I_{Na})	Sodium currents
(SCA27)	Spinocerebellar ataxia 27

References

1. Smallwood PM, Munoz-Sanjuan I, Tong P, Macke JP, Hendry SH, Gilbert DJ, Copeland NG, Jenkins NA, Nathans J. Fibroblast growth factor (fgf) homologous factors: New members of the fgf family implicated in nervous system development. Proc Natl Acad Sci U S A. 1996; 93:9850–9857. [PubMed: 8790420]
2. Munoz-Sanjuan I, Smallwood PM, Nathans J. Isoform diversity among fibroblast growth factor homologous factors is generated by alternative promoter usage and differential splicing. J Biol Chem. 2000; 275:2589–2597. [PubMed: 10644718]
3. Olsen SK, Garbi M, Zampieri N, Eliseenkova AV, Ornitz DM, Goldfarb M, Mohammadi M. Fibroblast growth factor (fgf) homologous factors share structural but not functional homology with fgfs. J. Biol. Chem. 2003; 278:34226–34236. [PubMed: 12815063]
4. Liu C, Dib-Hajj SD, Waxman SG. Fibroblast growth factor homologous factor 1b binds to the c terminus of the tetrodotoxin-resistant sodium channel rnav1.9a (nan). J Biol Chem. 2001; 276:18925–18933. [PubMed: 11376006]
5. van Swieten JC, Brusse E, de Graaf BM, Krieger E, van de Graaf R, de Koning I, Maat-Kievit A, Leegwater P, Dooijes D, Oostra BA, Heutink P. A mutation in the fibroblast growth factor 14 gene is associated with autosomal dominant cerebellar ataxia [corrected]. Am J Hum Genet. 2003; 72:191–199. [PubMed: 12489043]
6. Misceo D, Fannemel M, Baroy T, Roberto R, Tvedt B, Jaeger T, Bryn V, Stromme P, Frengen E. Sca27 caused by a chromosome translocation: Further delineation of the phenotype. Neurogenetics. 2009; 10:371–374. [PubMed: 19471976]
7. Dalski A, Atici J, Kreuz FR, Hellenbroich Y, Schwinger E, Zuhlke C. Mutation analysis in the fibroblast growth factor 14 gene: Frameshift mutation and polymorphisms in patients with inherited ataxias. Eur J Hum Genet. 2005; 13:118–120. [PubMed: 15470364]
8. Laezza F, Gerber BR, Lou J-Y, Kozel MA, Hartman H, Marie Craig A, Ornitz DM, Nerbonne JM. The fgf14f145s mutation disrupts the interaction of fgf14 with voltage-gated na+ channels and impairs neuronal excitability. J. Neurosci. 2007; 27:12033–12044. [PubMed: 17978045]
9. Liu CJ, Dib-Hajj SD, Renganathan M, Cummins TR, Waxman SG. Modulation of the cardiac sodium channel nav1.5 by fibroblast growth factor homologous factor 1b. J Biol Chem. 2003; 278:1029–1036. [PubMed: 12401812]
10. Lou J-Y, Laezza F, Gerber BR, Xiao M, Yamada KA, Hartmann H, Craig AM, Nerbonne JM, Ornitz DM. Fibroblast growth factor 14 is an intracellular modulator of voltage-gated sodium channels. J Physiol. 2005; 569:179–193. [PubMed: 16166153]
11. Xu X, Marx SO, Colecraft HM. Molecular mechanisms, and selective pharmacological rescue, of rem-inhibited cav1.2 channels in heart. Circ Res. 2010; 107:620–630. [PubMed: 20616312]
12. Bursac N, Parker KK, Iravanian S, Tung L. Cardiomyocyte cultures with controlled macroscopic anisotropy: A model for functional electrophysiological studies of cardiac muscle. Circ Res. 2002; 91:e45–54. [PubMed: 12480825]
13. McSpadden LC, Kirkton RD, Bursac N. Electrotonic loading of anisotropic cardiac monolayers by unexcitable cells depends on connexin type and expression level. Am J Physiol Cell Physiol. 2009; 297:C339–351. [PubMed: 19494239]
14. Nguyen TP, Wang DW, Rhodes TH, George AL Jr. Divergent biophysical defects caused by mutant sodium channels in dilated cardiomyopathy with arrhythmia. Circ Res. 2008; 102:364–371. [PubMed: 18048769]
15. Benson DW, Wang DW, Dyment M, Knilans TK, Fish FA, Strieper MJ, Rhodes TH, George AL. Congenital sick sinus syndrome caused by recessive mutations in the cardiac sodium channel gene (scn5a). The Journal of Clinical Investigation. 2003; 112:1019–1028. [PubMed: 14523039]

16. Sato PY, Musa H, Coombs W, Guerrero-Serna G, Patino GA, Taffet SM, Isom LL, Delmar M. Loss of plakophilin-2 expression leads to decreased sodium current and slower conduction velocity in cultured cardiac myocytes. Circ Res. 2009; 105:523–526. [PubMed: 19661460]

17. Goetz R, Dover K, Laezza F, Shtraizent N, Huang X, Tchetchik D, Eliseenkova AV, Xu CF, Neubert TA, Ornitz DM, Goldfarb M, Mohammadi M. Crystal structure of a fibroblast growth factor homologous factor (fhf) defines a conserved surface on fhfs for binding and modulation of voltage-gated sodium channels. J Biol Chem. 2009; 284:17883–17896. [PubMed: 19406745]

18. Lowe JS, Palygin O, Bhasin N, Hund TJ, Boyden PA, Shibata E, Anderson ME, Mohler PJ. Voltage-gated nav channel targeting in the heart requires an ankyrin-g–dependent cellular pathway. The Journal of Cell Biology. 2008; 180:173–186. [PubMed: 18180363]

19. Winn MP, Conlon PJ, Lynn KL, Farrington MK, Creazzo T, Hawkins AF, Daskalakis N, Kwan SY, Ebersviller S, Burchette JL, Pericak-Vance MA, Howell DN, Vance JM, Rosenberg PB. A mutation in the trpc6 cation channel causes familial focal segmental glomerulosclerosis. Science. 2005; 308:1801–1804. [PubMed: 15879175]

20. Wang Q, Bardgett ME, Wong M, Wozniak DF, Lou J, McNeil BD, Chen C, Nardi A, Reid DC, Yamada K, Ornitz DM. Ataxia and paroxysmal dyskinesia in mice lacking axonally transported fgf14. Neuron. 2002; 35:25–38. [PubMed: 12123606]

21. Wittmack EK, Rush AM, Craner MJ, Goldfarb M, Waxman SG, Dib-Hajj SD. Fibroblast growth factor homologous factor 2b: Association with nav1.6 and selective colocalization at nodes of ranvier of dorsal root axons. J Neurosci. 2004; 24:6765–6775. [PubMed: 15282281]

22. Goldfarb M, Schoorlemmer J, Williams A, Diwakar S, Wang Q, Huang X, Giza J, Tchetchik D, Kelley K, Vega A, Matthews G, Rossi P, Ornitz DM, D'Angelo E. Fibroblast growth factor homologous factors control neuronal excitability through modulation of voltage-gated sodium channels. Neuron. 2007; 55:449–463. [PubMed: 17678857]

23. Xiao M, Xu L, Laezza F, Yamada K, Feng S, Ornitz DM. Impaired hippocampal synaptic transmission and plasticity in mice lacking fibroblast growth factor 14. Molecular and Cellular Neuroscience. 2007; 34:366–377. [PubMed: 17208450]

24. Laezza F, Lampert A, Kozel MA, Gerber BR, Rush AM, Nerbonne JM, Waxman SG, Dib-Hajj SD, Ornitz DM. Fgf14 n-terminal splice variants differentially modulate nav1.2 and nav1.6-encoded sodium channels. Mol Cell Neurosci. 2009; 42:90–101. [PubMed: 19465131]

25. Smits JPP, Eckardt L, Probst V, Bezzina CR, Schott JJ, Remme CA, Haverkamp W, Breithardt G, Escande D, Schulze-Bahr E, LeMarec H, Wilde AAM. Genotype-phenotype relationship in brugada syndrome: Electrocardiographic features differentiate scn5a-related patients from non-scn5a-related patients. Journal of the American College of Cardiology. 2002; 40:350–356. [PubMed: 12106943]

26. Van Norstrand D, Tester DJ, Medeiros-Domingo A, Cheng J, Tan B-H, Valdivia CR, Rubinos C, Srinivas M, Asimaki A, Saffitz JE, Makielski JC, Ackerman MJ. Abstract 13448: The cardiac sodium nav1.5 channelsome and sudden infant death syndrome. Circulation. 2010; 122:A13448.

27. Wang C, Wang C, Hoch EG, Pitt GS. Identification of novel interaction sites that determine specificity between fibroblast growth factor homologous factors and voltage-gated sodium channels. JOURNAL OF BIOLOGICAL CHEMISTRY. 2011; 286:24253–24263. [PubMed: 21566136]

28. Rusconi R, Scalmani P, Cassulini RR, Giunti G, Gambardella A, Franceschetti S, Annesi G, Wanke E, Mantegazza M. Modulatory proteins can rescue a trafficking defective epileptogenic nav1.1 na+ channel mutant. J. Neurosci. 2007; 27:11037–11046. [PubMed: 17928445]

29. Rivolta I, Abriel H, Tateyama M, Liu H, Memmi M, Vardas P, Napolitano C, Priori SG, Kass RS. Inherited brugada and long qt-3 syndrome mutations of a single residue of the cardiac sodium channel confer distinct channel and clinical phenotypes. J. Biol. Chem. 2001; 276:30623–30630. [PubMed: 11410597]

Novelty and Significance

What is Known?

- Fibroblast growth factor homologous factors (FHFs), a subfamily of fibroblast growth factors (FGFs) do not function as traditional FGFs.
- FHFs are intracellular modulators of voltage-gated Na^+ channels and have been linked to neurodegenerative diseases.
- Certain FHFs have been found in embryonic heart

What New Information Does This Article Contribute?

- FGF13 (FHF2) is the dominant FHF present in murine ventricular myocytes
- FGF13 binds directly to, and co-localizes with the major cardiac Na^+ channel, $Na_V1.5$ in the sarcolemma of adult mouse ventricular myocytes.
- Knockdown of FGF13 in adult mouse ventricular myocytes results in a loss-of-function of NA^+ V1.5 characterized by reduced Na current (I_{Na}) density, decreased Na^+ channel availability, and slowed I_{Na} recovery from inactivation.
- Knockdown of FGF13 decreases $Na_V1.5$ at the sarcolemma but does not reduce whole-cell $Na_V1.5$ protein nor $Na_V1.5$ mRNA levels
- Knockdown of FGF13 slowed conduction velocity and reduced maximum capture rate in neonatal rat ventricular myocyte monolayers

FHFs are potent regulators of voltage-gated Na^+ channels and are expressed in embryonic heart, but whether they are also present in adult heart, regulate endogenous cardiac Na^+ channels, or participate in cardiac pathophysiology has not been explored. We discovered that the FHF FGF13 is the predominant FHF in adult murine ventricular myocytes, in which FGF13 binds directly to the Na 1.5 Na^+ V channels and modulates their function. Knockdown of FGF13 affected multiple Na^+ channel properties, including the amount of Na^+ current, kinetics of channel gating, trafficking of Na^+ channels to the sarcolemma, and conduction velocity through cardiac tissue. These newly identified roles for FHFs in adult ventricular myocytes suggest that loss-of-function mutations in FHFs may underlie cardiac arrhythmias and cardiomyopathies.

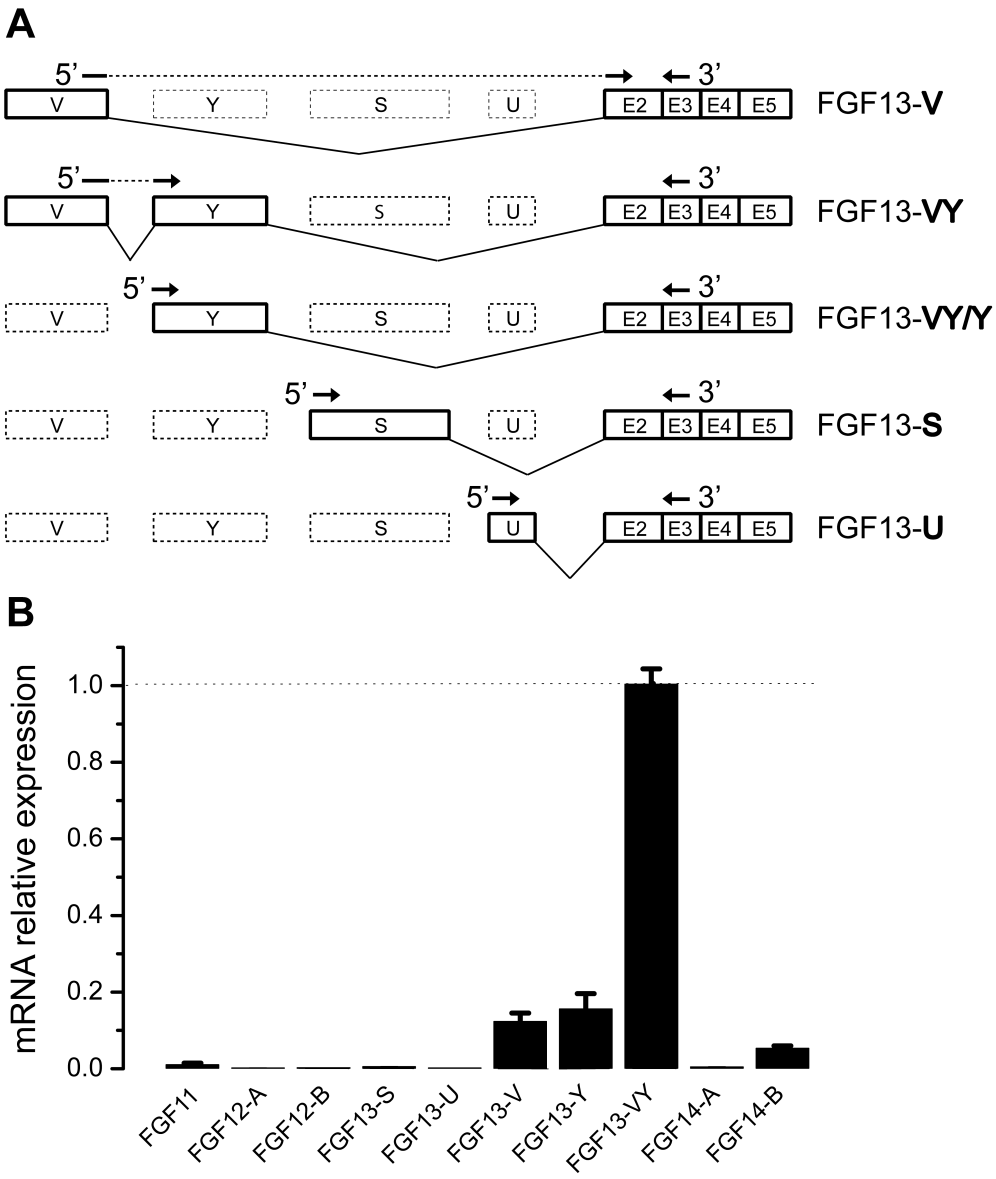

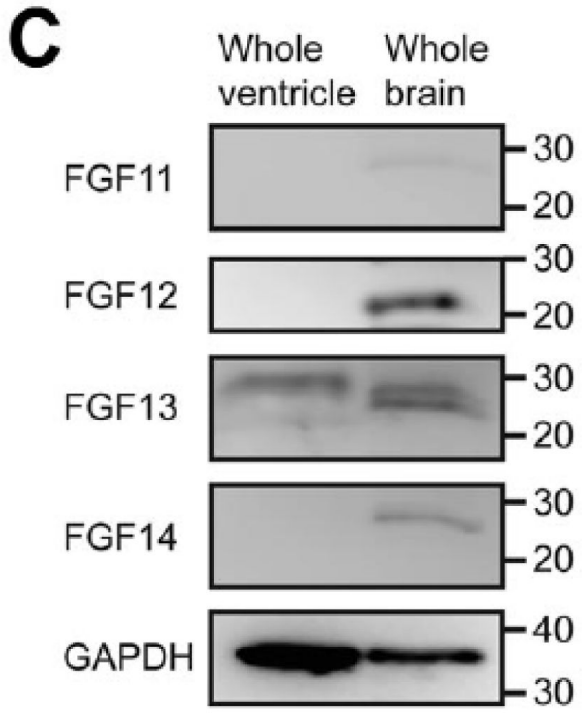

Figure 1.

FGF13 is the major FHF in mouse cardiac myocytes. (A) Schematic diagram of FGF13 splice variants and primers (arrows) used for qPCR of specific variants. The alternatively spliced first exons are shown in boxes labeled V, Y, S and U. Transcript levels for the other FHF family membranes were quantified using a similar strategy. (B) Relative mRNA expression of FGF11-14 in isolated adult mouse ventricular myocytes. All data were corrected with GAPDH and normalized to FGF13-VY. FGF13-Y relative levels were calculated by subtracting FGF13-VY from the sum of both FGF13-VY and FGF13-Y. Results were averaged from three different experiments. (C) Assessment of protein expression of the four FHF family members by immunoblot with FGF11-14 antibodies on isolated adult mouse ventricular myocytes and whole brain lysates. GAPDH was used as a loading control. Equal amounts of lysates (~30 μg for ventricular myocytes and ~15 μg for brain) were probed in each replicate.

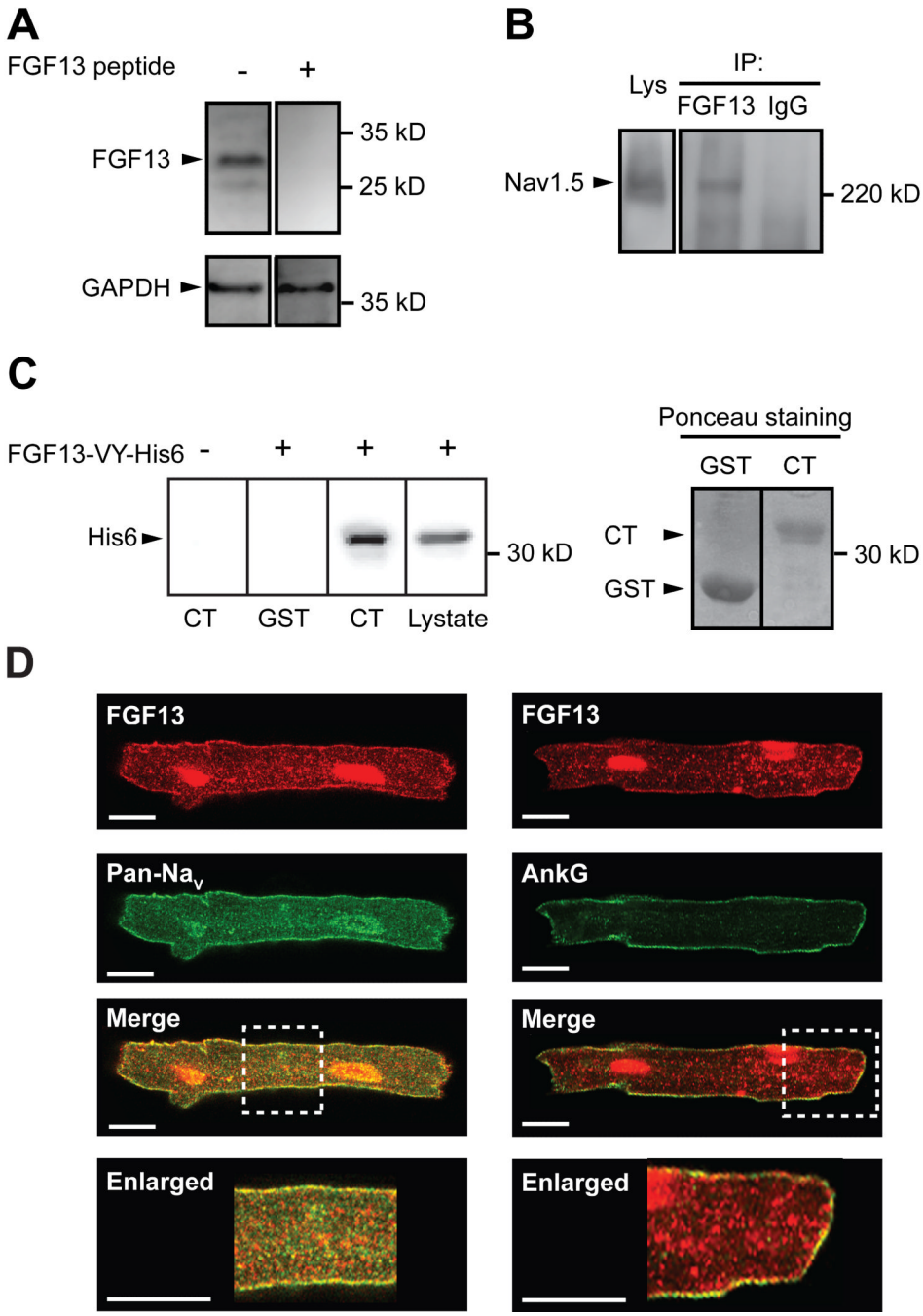

Figure 2.

FGF13 interacts directly, and co-localizes with $Na_V1.5$ in adult mouse ventricular myocytes lysates. (A) Detection of endogenous FGF13 in mouse ventricle by immunoblot with an FGF13 antibody or FGF13 antibody plus the immunizing FGF13 peptide antigen. GAPDH was used as loading control. (B) FGF13 co-immunoprecipitated with $Na_V1.5$. (C) Immunoblot of cell lysates with a His6 antibody, showing pull-down by GST-$Na_V1.5$ C-terminus (CT) of FGF13-VY-His6 expressed in tsA201 cells. On right, Ponceau staining of an example membrane used for His6 immunoblot demonstrates equal loading of the GST fusion proteins used in the pull down experiment: GST control (GST) or GST-$Na_V1.5$ CT (CT). (D) Confocal images of immunocytochemistry of FGF13 and $Na_V1.5$ (left panels) or

FGF13 and ankyrin-G (AnkG) (right panels) in adult mouse ventricular myocytes. Enlarged images (bottom panels) represent the boxed regions in the images above. Scale bar, 25 μm.

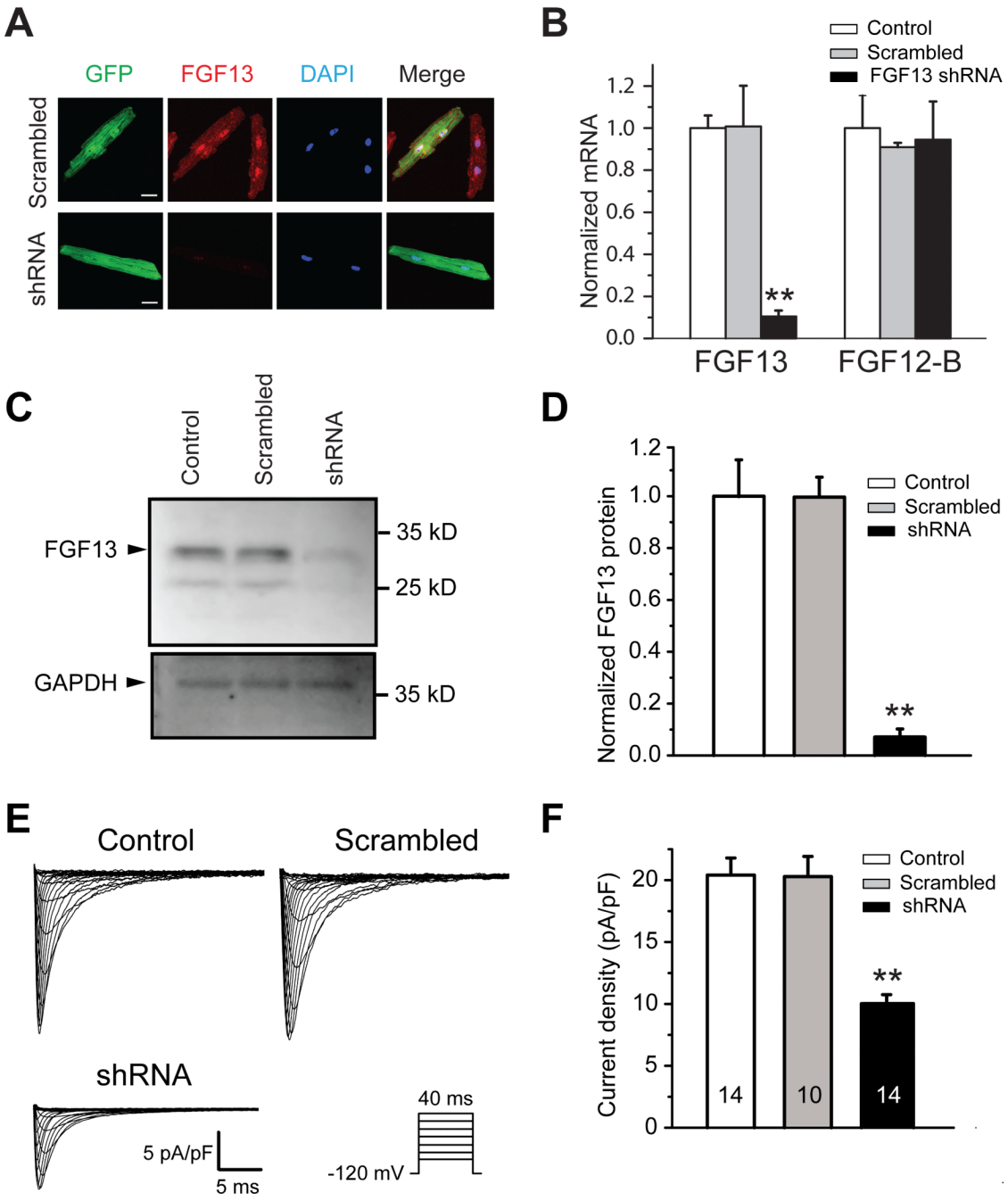

Figure 3.

Specific knockdown of FGF13 by shRNA decreases Na^+ channel current in adult mouse ventricular myocytes. (A) Confocal images of immunocytochemistry of FGF13 (red) after infection with adenovirus expressing FGF13 shRNA (bottom panels) or a Scrambled control (top panels) in ventricular myocytes. Infected myocytes were identified by GFP expression. Nuclei are stained with DAPI. Scale bar, 25 μm. (B) Quantitative analysis of FGF13 (using primers in the FGF-like core designed to amplify all FGF13 isoforms; see Online Table I) and FGF12B mRNA levels by qPCR in uninfected cultured myocytes (Control) or those infected with scrambled shRNA (Scrambled) or FGF13 shRNA (shRNA). All data were corrected with GAPDH and normalized to Control. **p<0.01, compare to control; n=6 for

FGF13 and n=3 for FGF12-B. (C) Representative immunoblot of FGF13 protein expression in isolated control myocytes, or myocytes infected with Scrambled or shRNA. Result is representative of three independent experiments. (D) Histograms showing normalized amounts of FGF13 protein from Control, Scrambled, or shRNA treated myocytes. $^{**}p<0.01$, compared to control; n=3. GAPDH was used as loading control. (E) Exemplar Na^+ channel current traces elicited by 40 ms depolarizing pulses to test potentials between −100 mV to +60 mV from a holding potential of −120 mV at 5 mV increments (Interpulse interval, 3 seconds). Inset shows schematic of the voltage-clamp protocol. (F) Means ± s.e.m. of maximum peak Na^+ channel current density measured at −30 mV in Control, Scrambled or shRNA infected myocytes. Numbers of cells tested are shown inside of each column. $^{**}p<0.01$, compared to control.

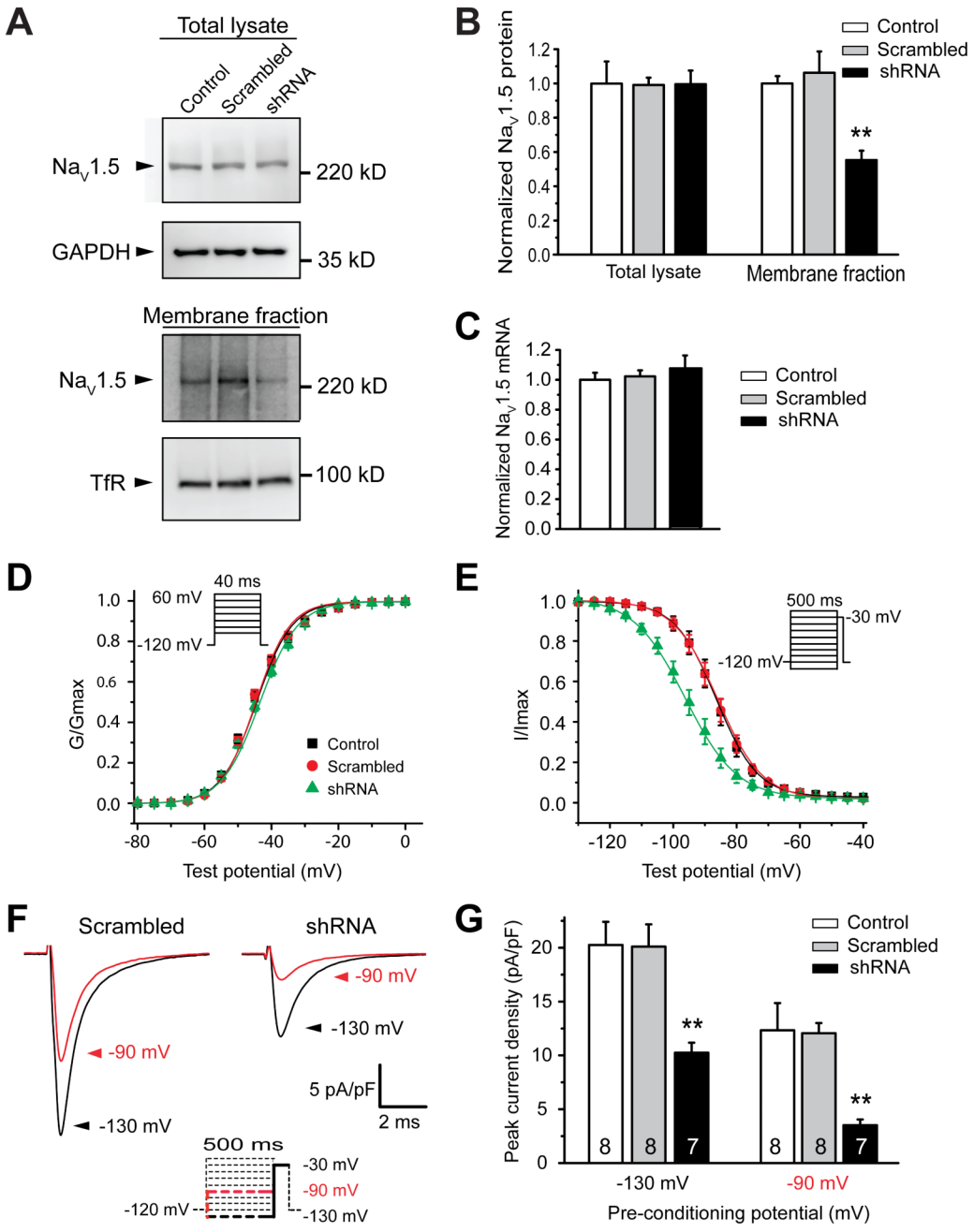

Figure 4.

Knockdown of FGF13 by shRNA decreases cell surface Na^+ channel levels and reduces channel availability in adult mouse ventricular myocytes. (A) Representative cell surface biotinylation experiment showing total $Na_V1.5$ (total lysate, top panels) and biotinylated $Na_V1.5$ (membrane fraction, bottom panels) in Control, Scrambled and FGF13 shRNA infected myocytes. GAPDH and transferrin receptor (TfR) were used as loading control for whole lysate and membrane fraction, respectively. No GAPDH was detected in the biotinylated fraction (not shown). Results are representative of three independent experiments. (B) Histograms showing the normalized amounts of total $Na_V1.5$ protein (total lysate) or biotinylated $Na_V1.5$ protein (membrane fraction) in myocytes of control,

scrambled or shRNA. Data were corrected with the loading control (GAPDH or TfR for total lysate or membrane fraction, respectively). $^{**}p<0.01$, compared to control. n=3. (C) Quantitative analysis of $Na_V1.5$ mRNA by qPCR in Control, Scrambled and shRNA infected myocytes. All data were corrected with GAPDH and normalized to Control. ** p<0.01, compare to control; n=6. (D) Voltage dependence of steady-state activation. (E) Voltage dependence of steady-state inactivation. See Table 2 for parameters. (F) Exemplar Na^+ channel current traces from Scrambled (left panel) and FGF13 shRNA (right panel) infected myocytes. Current traces are from a 20 ms test pulse at −30 mV elicited after a 500 ms pre-conditioning pulse at −130 mV (black) or −90 mV (red). The voltage protocol is shown in the inset. The pulse protocol cycle time was 3 seconds. (G) Histograms showing mean ±s.e.m. of Na^+ channel peak current density measured at a test pulse of −30 mV from pre-conditioning pulse of −130 mV (left panel) or −90 mV (right panel) in Control, Scrambled or shRNA infected myocytes. Numbers of cells tested are shown inside of each column. $^{**}p<0.01$, compared to control.

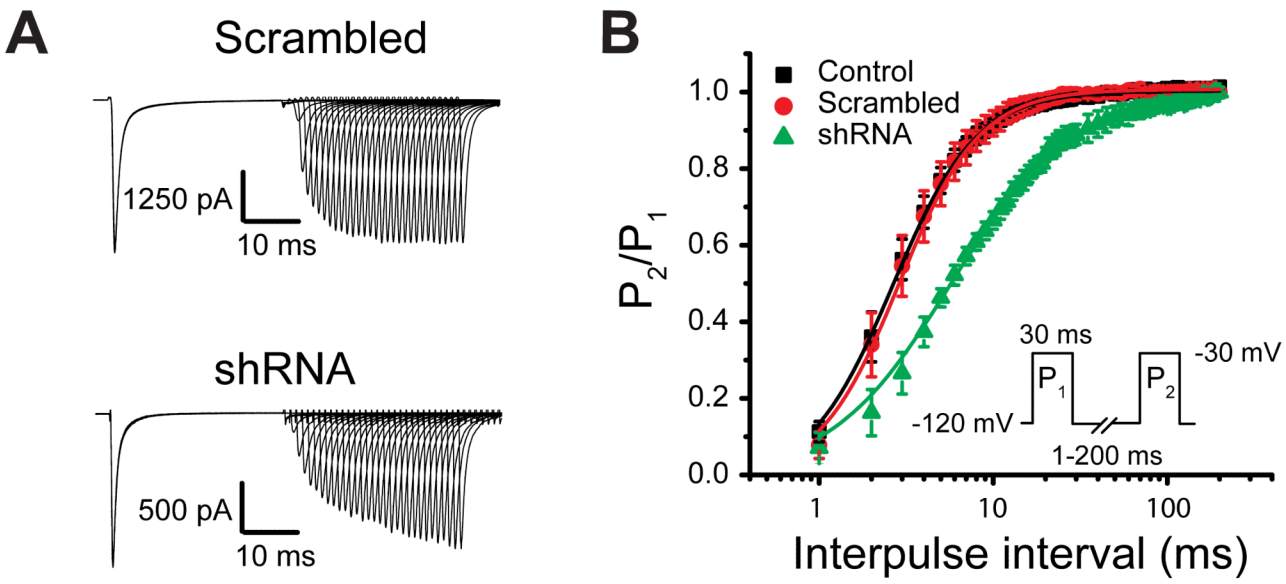

Figure 5.

Knockdown of FGF13 by shRNA slows Na^+ channel recovery from fast inactivation in adult mouse ventricular myocytes. (A) Exemplar current traces recorded in Scrambled (top panel) or shRNA (bottom panel) infected myocytes in response to voltage commands consisting of two −30 mV depolarization pulses (P_1 and P_2) from a holding potential of −120 mV, separated by 1 – 200 ms variable interpulse interval (P_1-P_2 interval) at −120 mV. The pulse protocol cycle time was 3 second. (B) Normalized I_{Na} recovery (P_2/P_1) versus interpulse interval at −120 mV in Control, Scrambled, and shRNA infected myocytes. Mean data were fitted by a double exponential and time constants of recovery are summarized in Table 2. Pulse protocol is shown in inset.

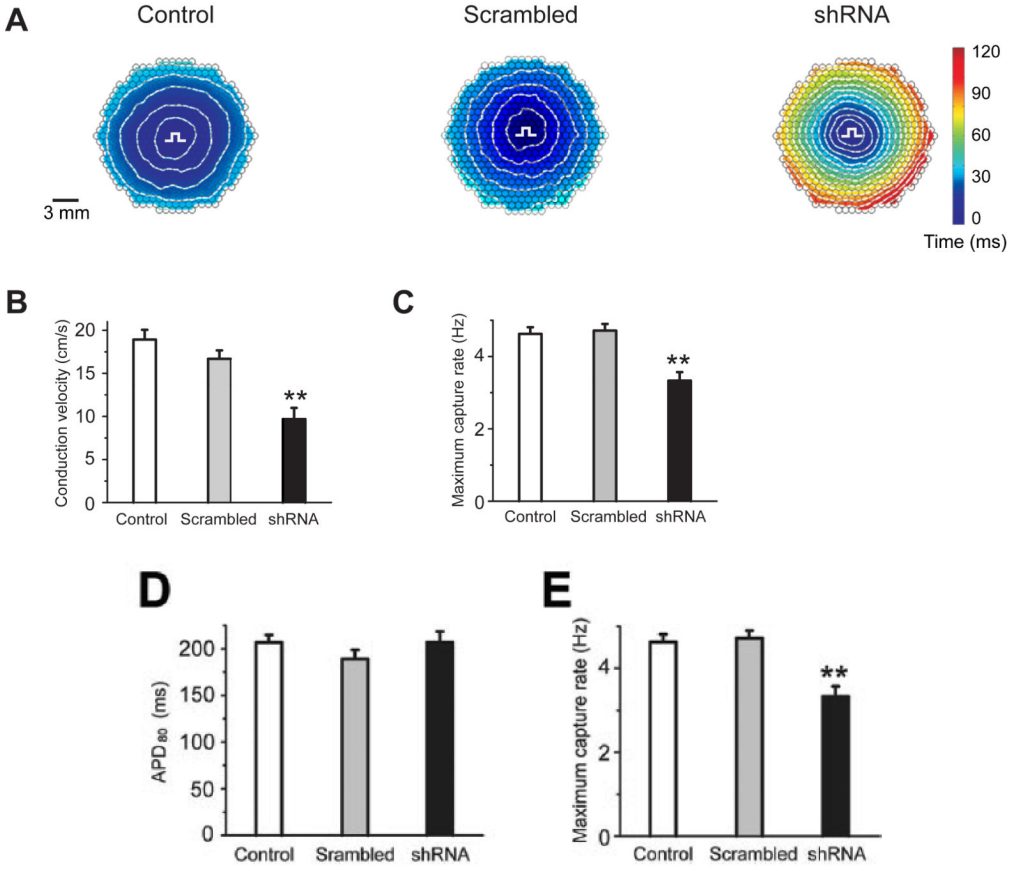

Figure 6.

Knockdown of FGF13 decreases conduction velocity and maximum capture rate in neonatal rat ventricular myocyte monolayers cultured on fibronectin. (A)-(B) Representative isochrone maps and action potential traces from uninfected (Control) monolayers or those infected with either Scrambled or FGF13 shRNA (shRNA). Data were obtained during 1 Hz point electrode stimulation (white pulse sign, π). (C)-(E) Calculated average conduction velocity, average action potential duration measured at 80% repolarization (APD_{80}), and average maximum capture rate (respectively). ** $p<0.001$, compared to control; n = 8, 7 and 9 for Control, Scrambled and shRNA infected myocytes, respectively.

Table 1

Summary of Electrophysiological Data

Parameter	Control	Scrambled shRNA	FGF13 shRNA
C_m (pF)	158.1 ± 8.9 (14)	155.7 ±12.7 (10)	154.4 ± 12.0 (14)
R_s (MΩ)	6.2 ± 0.4 (14)	6.5 ± 0.5 (10)	6.4 ± 0.3 (14)
I_{Na}-peak activation at −30 mV (pA/pF)	20.4 ± 1.4 (14)	20.3 ± 1.6 (10)	10.0 ± 1.8** (14)
I_{Na}-peak inactivation at −90 mV (pA/pF)	12.3 ± 2.5 (8)	12.1 ± 0.9 (8)	3.5 ± 0.3** (7)
I_{Na}-peak inactivation at −130 mV (pA/pF)	20.3 ± 2.1 (8)	20.1 ± 2.1 (8)	10.3 ± 0.9** (7)
$V_{1/2}$ of activation (mV)	−44.9 ± 0.6 (7)	−45.0 ± 0.5 (7)	−43.9 ± 0.5 (7)
***k* of activation (mV)**	6.1 ± 0.4 (7)	5.7 ± 0.4 (7)	6.3 ± 0.3 (7)
$V_{1/2}$ of inactivation (mV)	−86.7 ± 1.8 (8)	−86.7 ± 1.5 (8)	−95.5 ± 1.8** (7)
***K* of inactivation (mV)**	5.6 ± 0.2 (8)	6.3 ± 0.5 (8)	7.4 ± 0.7* (7)
τ-fast of recovery (ms)	3.1 ± 0.3 (12)	3.2 ± 0.4 (11)	9.0 ± 0.7** (6)
τ-fast amplitude (%)	94.5 ± 2.0 (12)	94.1 ± 1.9 (11)	82.1 ± 3.8** (6)
τ-slow of recovery (ms)	28.6 ± 3.2 (12)	29.8 ± 2.4 (11)	76.0 ± 6.1** (6)
τ-slow amplitude (%)	5.5 ± 2.0 (12)	5.9 ± 1.8 (11)	17.9 ± 3.8** (6)

The number for cells analyzed for each parameter is provided in parentheses.

* $p<0.05$

** $p<0.01$ compared to control.